

16. V. M. Burns and R. G. Burns, *Earth Planet. Sci. Lett.* **39**, 341 (1978); *Scanning Electron Microsc.* **1**, 245 (1978); *Am. Mineral.* **63**, 827 (1978).
17. M. Siegel, *Geol. Soc. Am. Abstr. Programs* **11**, 516 (1979).
18. The mineral ramsdellite (MnO₂) is included in the expanded version.
19. We thank D. Davis, J. Post, and D. Veblen for valuable discussion; V. Burns, S. Crane, G. Rossman, and the Smithsonian Institution for

kindly supplying samples for this project; and J. Wheatley for assistance in the electron microscope laboratory in the Center for Solid State Science at Arizona State University. The research was supported in part by grants EAR 77-00128 and EAR 79-26375 from the Earth Sciences Division of the National Science Foundation.

17 June 1980; revised 5 September 1980

Erosion of Galilean Satellite Surfaces by Jovian Magnetosphere Particles

Abstract. *The Galilean satellites of Jupiter—Io (J1), Europa (J2), Ganymede (J3), and Callisto (J4)—are embedded in the intense ion and electron fluxes of the Jovian magnetosphere. The effect of these particles on the icy surfaces of the outer three satellites depends on the fluxes and the efficiency of the sputtering of water ice by such particles. Recent laboratory measurements provided data on the erosion of water ice by energetic particles and showed that it occurs much faster than would be expected from normal sputtering theory. The Voyager spacecraft encounters with Jupiter provided the first measurements of ion fluxes (energies ≥ 30 kiloelectron volts) in the vicinity of the Galilean satellites. Using the laboratory sputtering data together with particle measurements from the Voyager 1 low-energy charged particle experiment, the effects of erosion on the surfaces of J2 to J4 are estimated. It is shown that the surface of Europa could be eroded by as much as 100 meters over an eon (10^9 years). Column densities of water vapor that could be produced around the three satellites from particle bombardment of their surfaces are also calculated, and the sources and losses of oxygen in the gravitationally bound gas produced by sputtering or sublimation are estimated.*

The outer three Galilean satellites of Jupiter—Europa (J2), Ganymede (J3), and Callisto (J4)—are immersed deeply in the magnetosphere of the planet (1, 2). Reflectance spectra show the surfaces of these three satellites to be covered totally or partially with water ice (3). If there is no appreciable atmosphere or intrinsic magnetic field associated with any of the satellites, the charged particles that impact them will produce erosion of their surfaces. Considerations of this erosion process, as well as the erosion of ice grains in the interplanetary and interstellar media, led to the initiation of laboratory experiments to investigate the sputtering of water ice by charged particles. The surprising discovery was made that the erosion was far greater than expected on the basis of contemporary sputtering theory that successfully accounts for erosion of metallic surfaces (4). These early laboratory results were used, together with extrapolations (to lower energies) of the particle fluxes reported from the Pioneer 10 encounter with Jupiter, to estimate the ice removal rates from the Galilean satellite surfaces and the possible satellite atmospheric and magnetospheric effects associated with this removal (5). It was concluded that sputtering played a role at least comparable to that of other erosion processes.

The laboratory experiments on the

sputtering of water ice have been extended to lower energies (6) and possible mechanisms involved in the sputtering process have been discussed to explain the observed species, energy, and temperature dependence. These new laboratory results are used in this report, together with particle energy spectra measured by the low-energy charged particle (LECP) experiment (7) on Voyager 1, to provide substantially more accurate estimates of the expected erosion of the water ice-covered surfaces of the Galilean satellites.

Results from Earth-based observations and from instruments on Voyager 1 and Voyager 2 show the outer three Galilean satellites to have vastly different surface characteristics. Callisto is approximately 5 to 25 percent ice-covered (3, 8) and heavily cratered (9). Ganymede is 20 to 65 percent ice-covered (3) and less cratered than Callisto, with some linear surface features. Europa is nearly 100 percent ice-covered (3), crisscrossed by linear features, and essentially devoid of craters (9). The ice temperatures of Europa and Ganymede have been estimated as ~ 95 and ~ 103 K (10), respectively, substantially colder than the full-disk brightness temperatures of ~ 124 and 135 K, respectively (11). In this report we consider these upper and lower limits on the average

temperatures. The characteristics of the surface of J2 may result from the Galilean satellite equivalent of tectonic processes. However, aspects of the smooth surface may also result from particle bombardment of the surface, as noted by the Voyager 2 imaging experiment team (9) and discussed below.

During the interval when Voyager 1 crossed the orbit planes of the Galilean satellites, the LECP experiment was in its planetary near-encounter mode in order to measure the most intense particle fluxes. The data used here were obtained by the low-energy magnetosphere particle analyzer (LEMPA) subsystem, which cannot separate ion species. However, from data taken before switching into this mode, just outside the orbit of J4 when ion species were being separately identified and counted by the low-energy particle telescope (LEPT) subsystem, we know that the ratio of fluxes of heavy ions (oxygen and sulfur) to the fluxes of protons and helium was rapidly increasing with decreasing distance from Jupiter (2, 12). This would be expected in view of satellite contributions to the magnetosphere ion fluxes, such as the sputtering discussed here, and the volcanoes of Io (J1). The erosion rates discussed in this report are calculated as lower (upper) limits, assuming that all of the ions incident on a satellite surface are protons (oxygen).

Plotted in the inset to Fig. 1a are the differential ion fluxes $dJ(E)/dE$ (where J is the flux of ions of energy E) measured on Voyager 1 by LEMPA. These fluxes are used to calculate the water ice erosion flux $\Phi(\text{H}_2\text{O})$ ($\text{cm}^{-2} \text{sec}^{-1}$) for the satellites, assuming each is 50 percent ice-covered

$$\Phi_i(\text{H}_2\text{O}) = 0.5 \int_0^\infty \frac{dJ}{dE} S_i(E) dE d\Omega \quad (1)$$

where $S_i(E)$ is the laboratory water ice "sputtering" coefficient measured for incident ion species i . The proton erosion coefficient S_H increases from ~ 0.2 to ~ 2 for a decrease in incident proton energy from ~ 1.5 to ~ 0.1 MeV; it then decreases to ~ 0.8 for a proton energy of ~ 6 keV (6). The erosion coefficient varies as the square of the incident particle electronic energy loss $[(dE/dx)^2]$ in the water ice for energies greater than ~ 1 keV per atomic mass unit. At lower energies collision cascade dominates. The oxygen erosion coefficient S_O is $\sim 150 \times S_H$ in the energy region where both have been measured and is assumed to have the same $(dE/dx)^2$ energy dependence at the higher energies. The sputtering also increases rapidly with in-

creasing surface temperature (6) above ~ 90 K. Here we ignore this and therefore our results are lower bounds on the erosion yields.

The ion fluxes dJ/dE at J3 and J4 were assumed constant below 30 keV when computing Eq. 1; this would place a lower bound on the yield. The ion fluxes at J2 were extrapolated from 100 to 30 keV by using the measured spectral form of the fluxes at J3. Near J1 and J2 the lower energy (≈ 100 keV) ion channels of the LEMPA detector were strongly affected by amplitude-dependent dead time, for which some corrections have been made. The uncertainties in the ion fluxes thus arise from three sources: (i) ion species, an uncertainty that is bounded by our considerations of hydrogen and oxygen; (ii) flux extrapolation from a lowest observed particle energy threshold of ~ 30 keV; and (iii) assumption of identical spectral form below 30 keV at J2 and J3.

We believe that the magnitude of the aggregate of these uncertainties does not exceed the uncertainty in actual particle access to a satellite surface arising from a possible tenuous atmosphere or a weak magnetic field. Finally, in calculating the eroded flux at each satellite, each surface was assumed to be uniformly bom-

barded by particles of all energies. Corrections to allow for corotation of the magnetosphere past a satellite were small compared to other uncertainties.

Figure 1a shows $\Phi(\text{H}_2\text{O})$ for each of the satellites, using S_{H} and S_{O} in Eq. 1. Also plotted as a function of temperature is $\Phi(\text{H}_2\text{O})$ due to sublimation, assuming a surface completely frost-covered. If the ice temperatures are those determined by Fink and Larson (10), particle erosion dominates sublimation for all three satellites for both incident hydrogen and oxygen. Even if the daytime ice temperatures correspond to the surface brightness temperatures (11), sputtering still dominates over most of the satellites' surfaces. Further, the sputtered particles are "hotter" than sublimed particles and therefore most important in determining surface losses (see below). We note that an H_2O erosion rate of $\sim 10^{10} \text{ cm}^{-2} \text{ sec}^{-1}$ over an eon (10^9 years) implies total erosion over this time of an ice layer ~ 100 m thick, which would greatly alter major icy features on a satellite surface. Such an erosion rate on Europa would be consistent with the implanted sulfur results inferred from International Ultraviolet Explorer data (13).

As yet, we do not have laboratory

results on the composition of the eroded species or their velocity distributions. The experiments do show that the water is eroded; no hydrogen or oxygen is preferentially left on a surface. Because the experimental erosion is so large, especially for incident oxygen, it is likely that most of the ice leaves a satellite surface as molecular clumps or H_2O molecules (4). In the following we assume they are molecules or dissociated molecular species.

The sputtered H_2O molecules will either escape from the satellite or be reabsorbed on the surface at another point. Molecules that are eventually reabsorbed will form a tenuous "atmosphere" around the satellite. The fraction undergoing either process depends on the energy of the sputtered products expressed as an effective temperature (kT) and on the sticking coefficient for reabsorbed particles. Based on ballistic trajectories, the atmospheric column density N of H_2O molecules per square centimeter is given as (14)

$$N = \frac{2}{\kappa} \frac{(2\pi MkT)^{1/2}}{Mg} \Phi_{\text{net}} \quad (2)$$

where $\Phi_{\text{net}} = \Phi_{\text{sputtered}} - \Phi_{\text{escape}}$, κ is the sticking coefficient, the molecular weight $M = 18$, and g is the acceleration due to gravity. Escape from the surface, Jeans escape, is determined by the velocity distribution of the sputtered particles; $\Phi_{\text{escape}} = (\Phi_{\text{sputtered}})(1 + \lambda_i) \times \exp(-\lambda_i)$, where $\lambda_i = E_{\text{escape}}/kT$ and E_{escape} is the minimum energy required for escape for H_2O molecules. The column density for a partially dissociated atmosphere is plotted in Fig. 1b for J2, J3, and J4 for assumed incident hydrogen and oxygen ions for the case of $\kappa = 0.5$ and a temperature of 2000 K [0.17 eV, based on estimates for other insulating materials (15)]. Also shown is the equilibrium vapor pressure of ice as a function of the ice temperature. The sputtered ion contribution dominates the H_2O column density produced by sublimation at each of the satellites for the expected ice temperatures given in Fink and Larson (10) and dominates over the majority of the surface for the higher temperature estimates.

Before the Voyager encounter, a stellar occultation measurement had suggested an atmospheric pressure as large as 10^{-3} mbar on Ganymede (16). Both sublimation (17) and sputtering (5) were proposed as the source of water for such an atmosphere. Voyager showed no atmosphere on Ganymede to a level of 10^{-8} mbar (18). Nevertheless, for theoretical purposes and comparison with observa-

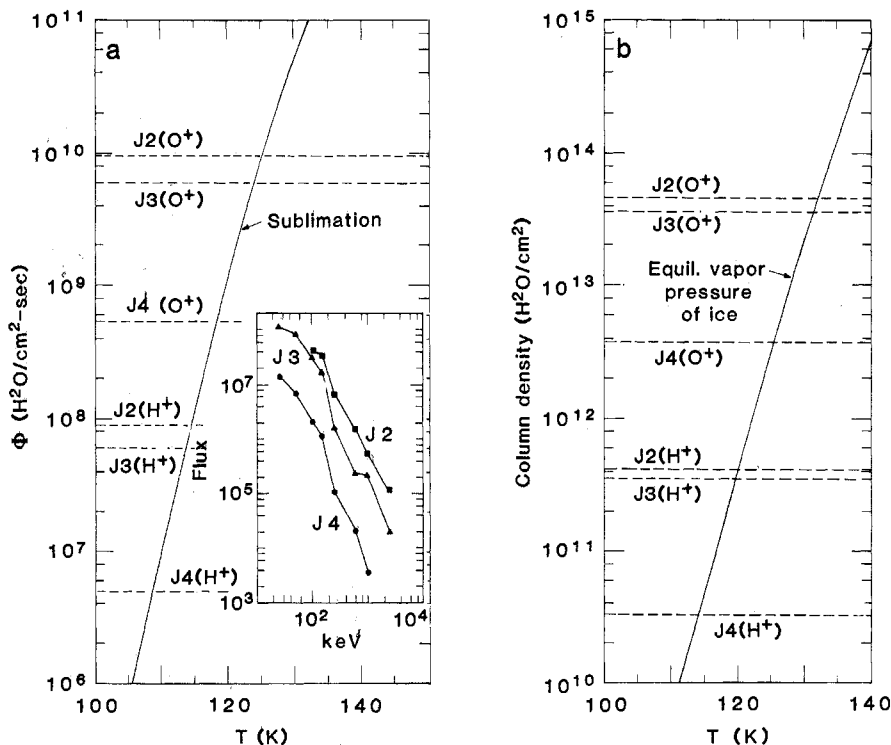


Fig. 1. (a) Comparison of H_2O sublimation flux for complete surface coverage to sputtered H_2O flux for incident hydrogen and oxygen over 50 percent of the surface. (Inset) Ion flux spectra (ions $\text{cm}^{-2} \text{sec}^{-1} \text{ster}^{-1} \text{MeV}^{-1}$) measured by the Voyager 1 LEP experiment. (b) Column density associated with the equilibrium vapor pressure of ice compared to column density of H_2O produced by sputtering, assuming the sputtered molecules have a temperature of 2000 K and a sticking coefficient of 0.5. Assumed surface coverage is 100 percent for sublimation, 50 percent for sputtering.

tion, it is of interest to compare the effectiveness of various processes that could produce an oxygen atmosphere on the Galilean satellites. We have done this for Ganymede; in Fig. 2 the column density of the atmosphere is plotted as a function of the oxygen flux for a variety of oxygen loss and source processes. Source curves 1 and 1' correspond to the Yung and McElroy (17) model of a Ganymede atmosphere, which is based on H₂O produced by sublimation at ~ 142 and ~ 135 K, respectively, in an O₂ atmosphere. For reference, source curves 5 and 5' correspond to the vaporization flux of H₂O with a satellite surface temperature of 120 and 110 K, respectively. Source curves 6 and 6' correspond to the sputtered flux at the satellite surface for 100 percent incident hydrogen and for 90 percent incident H⁺ plus 10 percent incident O⁺, respectively. Source curve 7 corresponds to dissociation of H₂O vapor by solar ultraviolet at the orbit of Jupiter, which chemically leads to the production of oxygen (17).

Loss curve 2 corresponds to oxygen escape arising from photodissociation of O₂ (15). Loss curve 3 corresponds to ionization by incoming protons (including charge exchange), electrons, and solar ultraviolet, with oxygen loss resulting from recombination or sweeping by the corotating magnetic field of Jupiter. Loss curves 4 and 4' estimate condensation on the satellite surface for $T = 2000$ K (0.17 eV), $\kappa = 0.1$, and $T = 10,000$ K (0.86 eV), $\kappa = 0.05$, respectively.

The Yung-McElroy column density for the atmosphere of Ganymede (17) can be determined by the intersection of the processes represented by lines 1 and 2 of Fig. 2. Such a column density would be reduced considerably by inclusion of ionization loss, which is predominantly due to incident particle radiation (curve 3 of Fig. 2). More importantly, it would be reduced drastically by a small surface temperature change, as noted earlier (5) (for instance, curve 1' crosses curves 2 and 3 in the region of 10^{14} to 10^{15} particles per square centimeter). Thus for average surface ice temperatures much colder than ~ 135 K, formation of a significant O₂ atmosphere by a sublimation source is very unlikely.

The largest single loss mechanism in a rarefied atmosphere consisting of a molecular or dissociated H₂O vapor is recondensation on a cold surface, as indicated by curves 4 and 4'. (The sticking coefficients are surely larger than assumed in the figure and depend on the fraction of the atmosphere dissociated.) Although for temperatures ≥ 115 K sublimation is the largest source of water

molecules, these are cool molecules and hence have even larger condensation rates. At temperatures below about 112 K on Ganymede, sputtering is the dominant source of H₂O in a rarefied atmosphere. With a mixture of 90 percent H⁺ and 10 percent O⁺ incident on the satellite surface, if the atoms and molecules are very hot and the sticking coefficient is very low (curve 4'), a column density of O₂ of $\sim 10^{14}$ cm⁻² can be expected on J3. Thus Figs. 1b and 2 indicate that for an ice temperature ≤ 135 K, an atmosphere column density $\geq 10^{15}$ cm⁻² is unlikely, which is consistent with the Voyager ultraviolet results (18).

In summary, we used measured Jovian magnetosphere ion fluxes from Voyager 1 and laboratory measurements of the erosion of water ice by hydrogen and oxygen ions to calculate removal rates of water ice on the surfaces of the Galilean satellites, which are immersed in Jupiter's magnetosphere. Further, we estimated the column densities of an atmosphere that could result from a particle erosion source. Finally, we estimated the source and loss processes for an

oxygen atmosphere around Ganymede as an example of the mechanisms that are operative at each of the three ice-covered Galilean satellites.

We note that our considerations of particle impact on the satellite surfaces could be altered by the existence of an intrinsic satellite magnetic field, as discussed for the Galilean satellites (19). An appreciable atmosphere would also limit the erosion rate (5), as indicated by curves 6 and 6' in Fig. 2. The existence of a satellite magnetic field would not totally exclude particles from impacting the satellite surfaces. Indeed, depending on the orientation of an assumed satellite dipole magnetic field with the local Jupiter magnetic field, as well as the efficiency of the interconnection of the magnetic fields, it is likely that the bombarding ions could impact a satellite surface in preferential locations. Such a selective bombardment might account for surface brightness variations. A combination of the results in this report with modeling of particle trajectories in satellite magnetic field geometries will help increase our understanding of the surface characteristics of the Galilean satellites.

R. E. JOHNSON

Department of Nuclear
Engineering and Engineering Physics,
University of Virginia,
Charlottesville 22901

L. J. LANZEROTTI
W. L. BROWN

Bell Laboratories,
Murray Hill, New Jersey 07974

T. P. ARMSTRONG
Department of Physics and Astronomy,
University of Kansas, Lawrence 66045

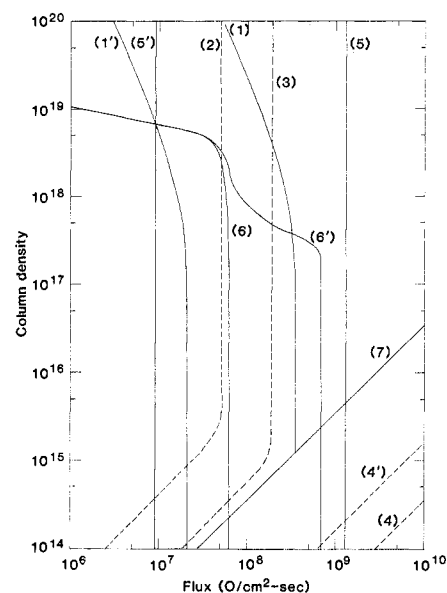


Fig. 2. Source (solid lines) and loss (dashed lines) processes for an oxygen atmosphere on Ganymede (J3). Curves represent (1) dissociation of H₂O from Yung and McElroy (17) atmosphere: 10^{-8} mbar H₂O, ~ 142 K in an O₂ atmosphere; (1') same as (1) for $T \sim 135$ K; (2) escape due to O₂ dissociation; (3) total ionization by Jovian protons, electrons, and solar ultraviolet; (4) condensation flux at surface for $T = 2000$ K, sticking coefficient = 0.1; (4') same as (4) for $T = 10^4$ K, sticking coefficient = 0.05; (5) vaporization flux of H₂O, surface $T \sim 120$ K; (5') same as (5) for $T \sim 110$ K; (6) sputtered flux for 100 percent incident H⁺; (6') sputtered flux for 90 percent incident H⁺ and 10 percent incident O⁺; and (7) dissociation of H₂O by ultraviolet.

References and Notes

1. J. A. Van Allen, D. N. Baker, B. A. Randall, M. F. Thomsen, D. D. Sentman, H. R. Flindt, *Science* **183**, 309 (1974); J. A. Simpson *et al.*, *ibid.*, p. 306; J. H. Trainor, B. J. Teegarden, D. E. Stilwell, F. B. McDonald, E. C. Roelof, W. R. Webber, *ibid.*, p. 311.
2. S. M. Krimigis *et al.*, *ibid.* **204**, 998 (1979).
3. C. B. Pilcher, S. T. Ridgway, T. B. McCord, *ibid.* **178**, 1087 (1972).
4. W. L. Brown, L. J. Lanzerotti, J. M. Poate, W. M. Augustyniak, *Phys. Rev. Lett.* **40**, 1027 (1978).
5. L. J. Lanzerotti, W. L. Brown, J. M. Poate, W. M. Augustyniak, *Geophys. Res. Lett.* **5**, 155 (1978).
6. W. L. Brown *et al.*, *Nucl. Instrum. Methods* **170**, 321 (1980); W. L. Brown, W. M. Augustyniak, L. J. Lanzerotti, R. E. Johnson, R. E. Evatt, *Phys. Rev. Lett.* **45**, 1632 (1980).
7. S. M. Krimigis, T. P. Armstrong, W. I. Axford, C. O. Bostrom, C. Y. Fan, G. Gloeckler, L. J. Lanzerotti, *Space Sci. Rev.* **21**, 329 (1977).
8. L. A. Lekofofsky, *Nature (London)* **269**, 785 (1977).
9. B. A. Smith *et al.*, *Science* **206**, 927 (1979).
10. U. Fink and H. P. Larson, *Icarus* **24**, 411 (1975).
11. D. Morrison, in *Planetary Satellites*, J. A. Burns, Ed. (Univ. of Arizona Press, Tucson, 1977), pp. 269-301; W. Sinton, *Int. Astron. Union Conf.* **57** (1980).
12. S. M. Krimigis *et al.*, *Science* **206**, 977 (1979).
13. A. L. Lane, R. M. Nelson, D. L. Matson, *Nature (London)*, in press.
14. See, for example, J. W. Chamberlain, *Theory of Planetary Atmospheres* (Academic Press, New York, 1978), chap. 7.

15. M. Szymoniski, H. Overijnder, A. E. de Vries, *Radiat. Eff.* **36**, 189 (1978).
16. R. W. Carlson *et al.*, *Science* **182**, 53 (1973).
17. Y. L. Yung and M. B. McElroy, *Icarus* **30**, 97 (1977).
18. A. L. Broadfoot *et al.*, *Science* **204**, 979 (1979).
19. F. Neubauer, *Geophys. Res. Lett.* **5**, 905 (1978).
20. A portion of the work at the University of Virginia was supported by NSF grant AST-79-12690. A portion of the work at the University of

Kansas was supported by subcontract from the Johns Hopkins University Applied Physics Laboratory, at which the LECP program is supported by NASA under task 1 of contract N00024-78-C5384 between Johns Hopkins University and the Department of Navy. We thank S. M. Krimigis of the Applied Physics Laboratory for profitable discussions.

16 September 1980; revised 19 January 1981

Interferon Action: RNA Cleavage Pattern of a (2'-5')Oligoadenylate-Dependent Endonuclease

Abstract. One of the mediators of interferon action is a latent endoribonuclease (ribonuclease L) that is activated by (2'-5')oligoadenylates. Among the homopolymers of the four common ribonucleotides, activated ribonuclease L degrades at an appreciable rate only polyuridylic acid. In two natural RNA's tested the most frequent ribonuclease L cleavages occur after UA, UG, and UU (A, adenine; U, uracil; and G, guanine) and much less frequent cleavages after CA and AC (C, cytosine).

Interferons are components of the antiviral and antitumor defenses of vertebrates. The treatment of cells with interferons is revealed in the cell extracts in several ways (1). Thus in an extract from interferon-treated cells (such as Ehrlich ascites tumor or HeLa cells) added messenger RNA is cleaved much

faster than in a corresponding extract from control cells. The faster cleavage requires adenosine triphosphate (ATP) and is manifested only if the extract is supplemented with double-stranded RNA (2). The enzyme system catalyzing the cleavage consists of two components (3). The first component is (2'-5')oligo-

adenylate synthetase, an enzyme induced by interferon, which if activated by double-stranded RNA converts ATP to (2'-5')oligoadenylates, such as (2'-5')pppApApA (4). This enzyme was purified to homogeneity and characterized (5, 6). The second component is ribonuclease L, a latent endoribonuclease, which can be activated by (2'-5')oligoadenylates (3, 7-9). The activation is reversible. It has been shown that on removal of (2'-5')oligoadenylates the enzyme returns to the latent state and on readdition of (2'-5')oligoadenylates it becomes reactivated (10). Here we present data on the unusual RNA cleavage pattern of the enzyme.

Partial purification of ribonuclease L by differential precipitation with ammonium sulfate and chromatography on DEAE-cellulose have been reported (10). Further purification by chromatography on phosphocellulose and poly(A)-agarose (11) increased the specific activity of the enzyme preparation about 14-fold. We have tested the cleavage preference of the ribonuclease L preparation first with poly(U) (polyuridylylate), poly(A) (polyadenylate), poly(C) (polycytidylylate), and poly(G) (polyguanylylate). Of

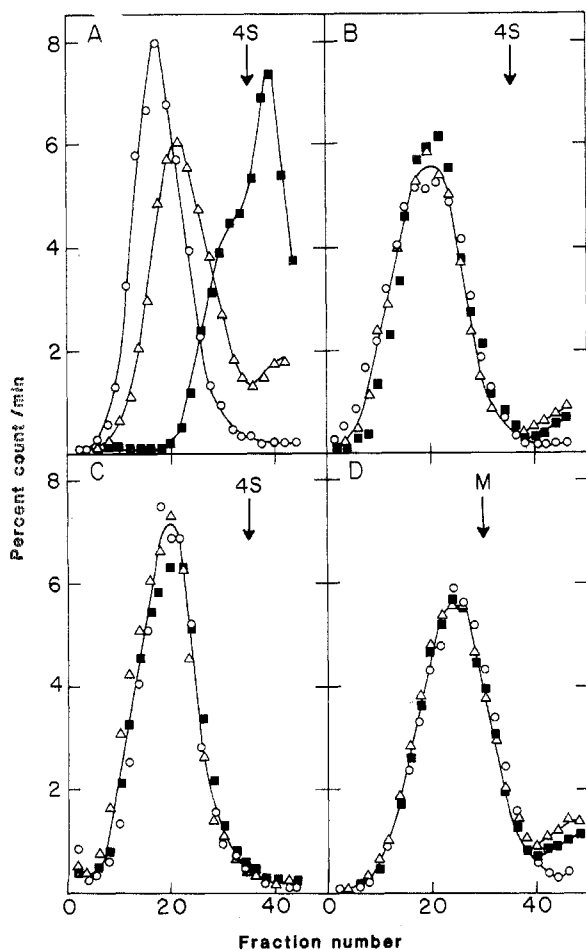


Fig. 1. RNA cleavage patterns of ribonuclease L: Experiments with homopolyribonucleotides. Ribonuclease L from Ehrlich ascites tumor cells was further purified from the DEAE-cellulose fraction of Slattery *et al.* (10) by chromatography on phosphocellulose and poly(A) agarose (11). The (2'-5')pppApApA was prepared according to Samanta *et al.* (6). [⁵-³H]Poly(U) (39 μ Ci per micromole of P), [⁸-³H]poly(A) (50.9 μ Ci per micromole of P), and [⁵-³H]poly(C) (41 μ Ci per micromole of P) were obtained from Miles Laboratories; [⁸-¹⁴C]poly(G) (3.2 μ Ci per micromole of guanine) and [⁸-¹⁴C]poly(A) (3 μ Ci per micromole of adenine) were obtained from P-L Biochemicals. Ribonuclease L was assayed as follows: the homopolyribonucleotide (50 μ g/ml) was incubated in buffer A, consisting of 25 mM tris-Cl, pH 8.2, 75 mM KCl, 5 mM magnesium acetate, and 10 mM β -mercaptoethanol without or with ribonuclease L (12 μ g/ml) and without or with (2'-5')pppApApA (1 μ M in adenosine monophosphate equivalents) in a final volume of 30 μ l at 30°C. After 10 minutes the reaction was terminated by the addition of 200 μ l of buffer B [10 mM tris-Cl, pH 7.5, 100 mM NaCl, 1 mM EDTA, 0.1 percent (weight to volume) sodium dodecyl sulfate], and a 200- μ l portion of the reaction mixture was applied on top of a 11.5-ml linear sucrose gradient [15 to 40 percent (weight to volume) in buffer B] and centrifuged at 177,000g at 15°C for 21 hours. In the analyses of experiments with [³H]poly(U), [³H]poly(C), and [¹⁴C]poly(G), *Escherichia coli* transfer RNA (0.25 μ g/ml) was used as an internal marker (sedimentation coefficient, 4S); in those with [³H]poly(A), the internal marker was [¹⁴C]poly(A) (sedimentation coefficient, 9S). Fractions (300 μ l) were collected and counted in a scintillation counter. (A) Experiments with poly(U); (B) experiments with poly(C); (C) experiments with poly(G); (D) experiments with poly(A). \circ , Incubation without ribonuclease L and (2'-5')pppApApA; Δ , incubation with ribonuclease L but without (2'-5')pppApApA; \blacksquare , incubation with both ribonuclease L and (2'-5')pppApApA. The locations in the gradients of tRNA (4S) and of 9S-[¹⁴C]poly(A) (M) are indicated by arrows. Percent count/min is the ratio of the net counts per minute in the fraction to the sum of the net counts per minutes in all fractions (the net counts per minute is the number of counts per minute in the fraction minus the background).